Multifractal Characterization of Soil Particle-Size Distributions

Adolfo N. D. Posadas, Daniel Giménez,* Marco Bittelli, Carlos M. P. Vaz, and Markus Flury

ABSTRACT

A particle-size distribution (PSD) constitutes a fundamental soil property correlated to many other soil properties. Accurate representations of PSDs are, therefore, needed for soil characterization and prediction purposes. A power-law dependence of particle mass on particle diameter has been used to model soil PSDs, and such power-law dependence has been interpreted as being the result of a fractal distribution of particle sizes characterized with a single fractal dimension. However, recent studies have shown that a single fractal dimension is not sufficient to characterize a distribution for the entire range of particle sizes. The objective of this study was to apply multifractal techniques to characterize contrasting PSDs and to identify multifractal parameters potentially useful for classification and prediction. The multifractal spectra of 30 PSDs covering a wide range of soil textural classes were analyzed. Parameters calculated from each multifractal spectrum were: (i) the Hausdorff dimension, $f(\alpha)$; (ii) the singularities of strength, α; (iii) the generalized fractal dimension, D_q; and (iv) their conjugate parameter the mass exponent, $\tau(q)$, calculated in the range of moment orders (q) of between −10 and +10 taken at 0.5 lag increments. Multifractal scaling was evident by an increase in the difference between the capacity D_0 and the entropy D_1 dimensions for soils with more than 10% clay content. Soils with <10% clay content exhibited single scaling. Our results indicate that multifractal parameters are promising descriptors of PSDs. Differences in scaling properties of PSDs should be considered in future studies.

A soil PSD is one of the fundamental properties characterizing a soil. Information on PSD defined as a combination of clay, silt, and sand contents, is often reduced to a textural class (Soil Survey Division Staff, 1993). Soils grouped in a textural class, however, exhibit a wide range of PSD, making the information contained in a textural triangle suitable only for general classification purposes.

Different functions are used to fit detailed experimental data on PSD (Buchan et al., 1993). Many of these functions are based on a power-law dependence of particle mass on particle diameter (Turcotte, 1986). Such power-law dependence has been interpreted as being the result of a fractal distribution characterized with a single fractal dimension (Matsushita, 1985; Turcotte, 1986; Tyler and Wheatcraft, 1992). Other results, however, have shown that a single fractal dimension is not sufficient to describe PSD in soil (Wu et al., 1993; Grout et al., 1998; Bittelli et al., 1999). Wu et al. (1993) combined several methods to obtain particle sizes ranging from 0.02 μm to several millimeters. They identify three domains with different power exponents. Bittelli et al. (1999), using the model of Turcotte (1986) and Tyler and Wheatcraft (1992), also found that three domains characterized the cumulative PSD of 19 soils. They associated the power exponent in each domain with fractal dimensions defining scaling in the clay, silt, or sand domains.

A distribution of particle sizes reflects the relative balance of weathering and pedogenetic processes. Primary minerals, generally present in the sand- and silt-size fractions, originate from weathering of a parent material, while clay minerals are the result of weathering and synthesis of new minerals. The different origin of the various size fractions may explain the various scaling domains observed in soil PSD (Wu et al., 1993; Bittelli et al., 1999). Grout et al. (1998) found that a single fractal dimension obtained from the model of Tyler and Wheatcraft (1992) did not describe adequately the distribution of particle sizes of three soils, and proposed multifractal techniques as a promising alternative to characterize PSD. Multifractal distributions may be best suited to represent the multiplicative action of the various pedogenetic processes acting on a parent material and resulting in a given distribution of particle sizes.

Multifractal methods have been applied in many areas of applied sciences. Muller and McCauley (1992) used multifractal for characterization of pore systems in rocks. Kropp et al. (1994) quantified spatial variability in bioactive marine sediments. Appleby (1996) characterized distribution patterns of the human population, and Cheng and Agterberg (1995) described the underlying spatial structure of Au mineral occurrence using multifractal models. On the other hand, there are few studies using multifractal methods to characterize soil properties. Most of the applications are related to the spatial variability of soil properties (e.g., surface strength) (Folorunso et al., 1994), hydraulic conductivity (Liu and Molz, 1997), and various soil properties (Kravchenko et al., 1999). Recently, Martin and Taguas (1998) suggested the entropy dimension, D_1, as a useful parameter for classifying soil texture within the classical textural triangle.

Grout et al. (1998) applied multifractal techniques to the study of PSDs, but their analyses were limited to three size distributions of mostly clayey soils. Without a more comprehensive study it is difficult to assess the applicability of the multifractal model to the description of PSD in soils.

The objective of this work was to apply multifractal methods to the characterization of contrasting soil PSDs, and to identify trends in the multifractal parameters related to textural separates.

Adolfo N.D. Posadas and Daniel Giménez, Dep. of Environmental Sciences, Rutgers Univ., 14 College Farm Road, New Brunswick, NJ 08901. Marco Bittelli and Markus Flury, Dep. of Crop and Soil Sciences, Washington State Univ., WA 99164. Carlos M.P. Vaz, Embrapa Agricultural Instrumentation Center, P.O. Box 741, 13560-970, São Paulo, S.P., Brazil. Received 25 July 2000. *Corresponding author (gimenez@envsci.rutgers.edu).

Published in Soil Sci. Soc. Am. J. 65:1361–1367 (2001).

Abbreviations: α, singularity of strength; $f(\alpha)$, Hausdorff dimension; D_0, capacity dimension; D_1, entropy dimension; D_2, correlation dimension; D_q, the generalized fractal dimension; PSD, particle-size distribution; $\tau(q)$, correlation exponent of the q^{th} order; q, moment order of a distribution.

Theory

Multifractal models provide more information about a distribution of a physical system than fractal models (Voss, 1988). A brief overview of multifractal theory is presented here, but more detailed discussions can be found in Feder (1988), Voss (1988), Evertsz and Mandelbrot (1992), and Gouyet (1996).

In a homogeneous system, the probability (P) of a measure varies with scale L as (Chhabra et al., 1989; Evertsz and Mandelbrot, 1992; and Vicsek, 1992):

$$P(L) \sim L^{D} \quad [1]$$

where D is a fractal dimension. For heterogeneous or nonuniform systems, the probability within the i^{th} region P_i scales as:

$$P_i(L) \sim L^{\alpha_i} \quad [2]$$

where α_i is the Lipschitz-Holder exponent or singularity strength, characterizing scaling in the i^{th} region (Feder, 1988). A technique to determine multifractal parameters is to cover a measure with boxes of size L. Similar α_i values can be found at different positions within a distribution. The number of boxes $N(\alpha)$ where the P_i has singularity strengths between α and $\alpha + d\alpha$ is found to scale as (Chhabra, et al., 1989; Hasley et al., 1986):

$$N(\alpha) \sim L^{-f(\alpha)} \quad [3]$$

where $f(\alpha)$ can be defined as the fractal dimension of the set of boxes with singularities α. The exponent α can take on values from the interval $[\alpha_{-\infty}, \alpha_{+\infty}]$, and $f(\alpha)$ is usually a single humped function with a maximum at $df(\alpha(q))/d\alpha(q) = 0$, where q is the moment order of a distribution. Thus, when $q = 0$, f_{max} is equal to the box-counting or D_0 (Gouyet, 1996; Viksec, 1992).

Multifractal sets can also be characterized on the basis of the generalized dimensions of the q^{th} moment orders of a distribution, D_q, defined as (Hentchel and Procaccia, 1983):

$$D_q = \frac{1}{q-1} \lim_{L \to 0} \frac{\log \mu(q,L)}{\log L}, \quad [4]$$

where $\mu(q, L)$ is the partition function defined as (Chhabra et al., 1989):

$$\mu(q,L) = \sum_{i=1}^{N(L)} P_i^q(L), \quad [5]$$

The generalized dimension D_q is a monotone decreasing function for all real q values within the interval $[-\infty, +\infty]$. When $q < 0$, μ emphasizes regions in the distribution with less concentration of a measure, whereas the opposite is true for $q > 0$ (Chhabra and Jensen, 1989).

The partition function scales as:

$$\mu(q, L) \sim L^{\tau(q)} \quad [6]$$

where $\tau(q)$ is the mass or correlation exponent of the q^{th} order defined as (Hasley et al., 1986; Viksec, 1992):

$$\tau(q) = (q-1) D_q \quad [7]$$

The connection between the power exponents $f(\alpha)$ (Eq. [3]) and $\tau(q)$ (Eq. [6]) is made via the Legendre transformation (Callen, 1985; Chhabra and Jensen, 1989; Hasley et al., 1986):

$$f(\alpha(q)) = q\alpha(q) - \tau(q) \quad [8]$$

and,

$$\alpha(q) = \frac{d\tau(q)}{dq}. \quad [9]$$

The $f(\alpha)$ spectrum and the generalized dimensions contain the same information, both characterizing interwoven ensemble of fractals of dimension $f(\alpha_i)$. In each of the i^{th} fractals, the observable P_i scales with the Lipschitz-Hölder-exponent α_i.

The generalized dimensions for $q = 0$, $q = 1$, and $q = 2$ are known as D_0, D_1, and the correlation dimension, D_2. The capacity dimension is independent of q and provides global (or average) information of a system (Voss, 1988). The D_1 is related to the information or Shannon entropy (Shannon and Weaver, 1949), and quantifies the degree of disorder present in a distribution, by measuring the way the Shannon entropy {i.e., $\Sigma\mu(L) \log[\mu(L)]$} scales as L tends to 0. According to Gouyet (1996) and Andraud et al. (1994, 1997) for a measure $\mu \in [0, 1]$, the value of D_1 is in the range of $0 < D_1 < 1$. A D_1 value close to 1.0 characterizes a system uniformly distributed throughout all scales, whereas a D_1 close to 0 reflects a subset of the scale in which the irregularities are concentrated. The D_2 is mathematically associated to the correlation function (Grassberger and Procaccia, 1983) and computes the correlation of measures contained in intervals of size L. The relationship between D_0, D_1, and D_2 is,

$$D_2 \leq D_1 \leq D_0$$

where the equality $D_0 = D_1 = D_2$ occurs only if the fractal is statistically or exact self similar and homogeneous (Korvin, 1992).

MATERIALS AND METHODS

Particle-Size Distributions

A total of 30 PSDs were analyzed. The database encompassed eight soils from the USA, 14 soils from Switzerland, and eight soils sampled from different regions of the state of São Paulo, Brazil. Five of the USA soils and the Swiss soils were taken from Bittelli et al. (1999). The remaining three PSDs from the USA soils were obtained for this study using a Leeds and Northrup MICROTRAC Standard Range particle-size Analyzer (SRA) (Microtrac, Inc., Montgomeryville, PA). The analyzer reads wet and slurry mixtures from 0.20 to 704 μm. Soil samples were crushed and placed in a muffle furnace at 600°C for 12 to 16 h to burn the organic matter, and then dispersed using sodium hexametaphosphate (NaHMP). Particle-size distributions in Bittelli et al. (1999), covering a size range from 0.12 to 1000 μm, were obtained using a small-angle light scattering apparatus. For the Brazilian soils, a gamma ray attenuation method was used to obtain distribution of particle sizes in the range from 2 to 250 μm (Vaz et al., 1992; Oliveira et al., 1997; Naime et al., 2001). Percentages of clay, silt, and sand of the soils in this study are summarized in Table 1, and their distribution in the textural triangle is shown in Fig. 1. The textural triangle shows three groups following an increase of either clay, silt, or sand while maintaining one of the fractions more or less constant (Fig. 1). Between 50 and 80 particle-size measurements were available in each PSD, covering the range from 0.5 to 250 μm (except for the Brazilian soils that were between 2.2 and 250 μm), with the largest concentration of measurements for particles smaller than 50 μm.

Determination of Multifractal Parameters

We followed the method developed by Chhabra and Jensen (1989) to calculate the $f(\alpha)$-spectrum because of its simplicity and accuracy when using experimental data. The distribution of a measure was evaluated within intervals of size L for different weights or moments q of the distribution. The normalized measure $\mu_i(q, L)$ was expressed as:

Table 1. Origin, soil classification, and soil textural composition of the 30 soils studied.

Soils		Soil classification†	Sand	Silt	Clay
			%		
Brazil	Dusk Red Latosol 1	Oxisol	18.0	0.8	81.2
	Dusk Red Latosol 2	Oxisol	24.7	21.9	53.4
	Dusk Red Latosol 3	Oxisol	31.0	13.6	55.4
	Red Yellow Latosol 1	Oxisol	44.1	11.4	44.5
	Red Yellow Latosol 2	Oxisol	35.5	20.8	43.7
	Red Yellow Podzolic 1	Ultisol	51.8	16.2	32.0
	Red Yellow Podzolic 2	Ultisol	58.9	24.9	16.2
	Red Yellow Podzolic 3	Ultisol	57.1	8.3	34.6
Switzerland	Affoltern	Typic Hapludalf	47.4	48.5	4.1
	Aeugst	Typic Hydraquent	38.7	55.6	5.7
	Buelach	Typic Hapludalf	57.2	40.4	2.4
	Les Barges	Mollic/Aquic Udifluvents	74.2	25.5	0.3
	Mettmenstetten	Lithic Ustorthent	55.6	40	4.4
	Murimoos	Lithic Medihemist	69.9	29.6	0.5
	Obermumpf	Lithic Rendoll	25.6	69.2	5.2
	Obfelden	Typic Hydraquent	36.3	59.6	4.1
	Reckenholz	Vertic/Typic Eutrochrept	23.8	70.7	5.5
	Rheinau	Arenic Eutrochrept	68.1	29.2	2.7
	Wetzikon 1	Lithic Ruptic-Alfic Eutrochept	48.9	46.7	4.4
	Wetzikon 2	Rendollic Eutrochept	59.7	37.2	3.1
	Wuelfingen	Vertic/Typic Eutrochrept	32.7	60.5	6.8
	Zeiningen	Ultic Hapludalf	40.5	55.4	4.1
USA	Gladstone	Typic Hapludults	46.9	41.9	11.2
	Holmdel	Aquic Hapludults	75.1	18.4	6.5
	Palouse	Ultic Haploxeroll	13.2	68.6	18.2
	Red Bluff	Ultic Palexeralfs	17.9	36.5	45.6
	Ryder	Ultic Hapludalfs	25.8	58	16.2
	Royal	Ultic Haploxeroll	30.7	63.1	6.2
	Salkum	Xeric Palehumults	11.9	59.7	28.4
	Walla Walla	Typic Haploxeroll	8.3	78.4	13.3

† U.S. soil taxonomy.

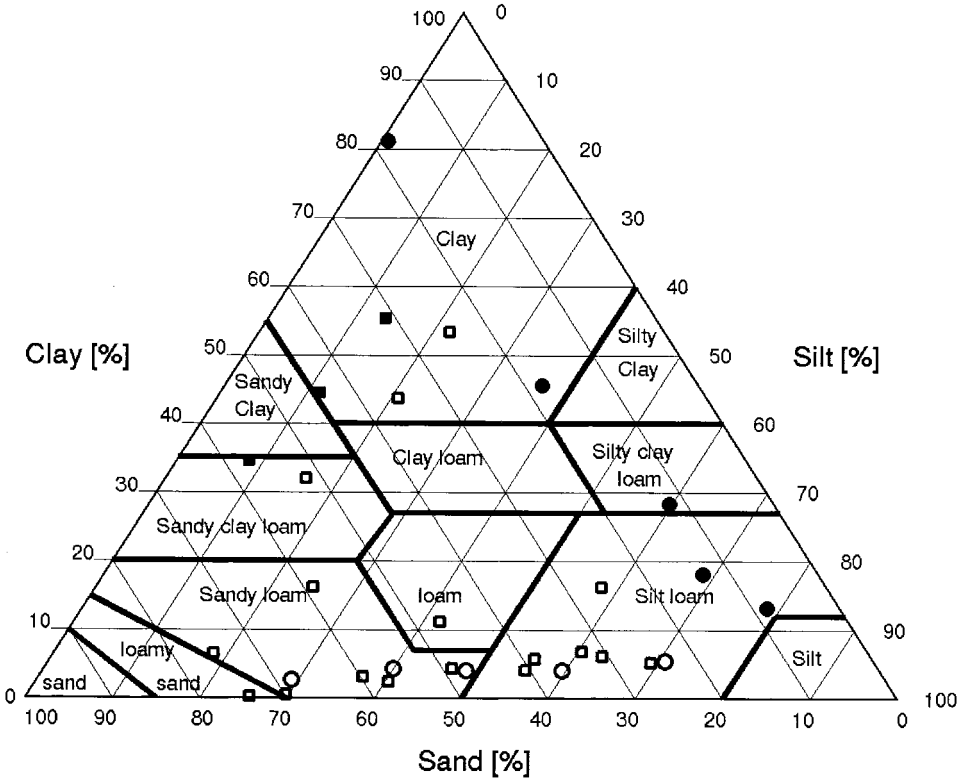

Fig. 1. Soil textural triangle according to the Soil Survey Division Staff (1993), showing the range of soils studied. Three groups of selected soils are distinguished based on variations in the content of two soil separates while keeping the third one approximately constant. Soils in Group 1 (○) vary along the silt and sand axis. Soils in Group 2 (■) vary along the clay and sand axis. Soils in Group 3 (●) vary along the silt and clay axis. Open squares represent all other soils in the database.

$$\mu_i(q, L) = \frac{P_i^q(L)}{\sum_{i=1}^{N(L)} P_i^q(L)} \quad [10]$$

where $P_i(L)$ is the probability of finding a class-i measure in the interval L. In our case, a PSD was partitioned in intervals of size L, and μ_i was constituted by the percentage of mass contained in each i^{th} interval. The multifractal spectrum, $f(q)$ vs. $\alpha(q)$, was calculated as in (Chhabra et al., 1989; Chhabra and Jensen, 1989):

$$f(q) = -\lim_{N\to\infty} \frac{1}{\log(N)} \sum_{i=1}^{N(L)} \mu_i(q,L)\log[\mu_i(q, L)] \quad [11]$$

$$\alpha(q) = -\lim_{N\to\infty} \frac{1}{\log(N)} \sum_{i=1}^{N(L)} \mu_i(q,L)\log[P_i(L)] \quad [12]$$

Cumulative mass size distribution curves were interpolated using a spline technique, and the amount of mass determined for each interval of size L. The total number of points used to compute a multifractal spectrum varied between 120 and 200. The maximum value of L that can be used in Eq. [11] and [12] and the range of q values was assessed by the linear behavior of the function $\Sigma_{i=1}^{N(L)} \mu_i (q, L) \log[\mu_i (q, L)]$ vs. $\log (L)$ for all the values of q used (Chhabra et al., 1989; Evertsz and Mandelbrot, 1992). The values of q considered were between –10 and +10 taken at 0.5 lag increments. In addition, we tested the validity of the results by verifying that the tangent of the graph $f(\alpha)$ vs. α at $\alpha = 1$ is the bisector defined by $df(\alpha)/d\alpha = q$. The point of intersection corresponds to $f[\alpha(1)] = \alpha(1) = D_1$ (Evertsz and Mandelbrot, 1992). The D_q and $\tau(q)$ were obtained with Eq. [7] and [8], respectively. The errors in the D_q's were estimated using the theory of propagation of error considering the square root of the error mean square (standard deviation) in Eq. [7] and [8] (Beers, 1953).

RESULTS AND DISCUSSION

Values of the regression coefficients, R^2, of the linear fit of the summation term of the right-hand-side of Eq. [11]$\{\Sigma_{i=1}^{N(L)} \mu_i (q, L) \log[\mu_i (q, L)]$ vs. $\log (L)\}$ were highest for $q = 0$ and $q = 1$ (Table 2) and decreased for higher q's. For most soils, the maximum value of L used was ~50 μm covered with ~25 steps. The R^2 varied between 0.988 and 0.999 for $q = 0$, and between 0.968 to 0.999 for $q = 1$ (Table 2). For samples with <10% clay, the R^2 dropped to about 0.6 for both $q = –10$ and $q = +10$. The drop of R^2 with higher q's was more pronounced for samples with >10% clay. For a homogeneous system, the summation term of the right-hand side of Eq. [11] is linear and with similar slopes for a wide range of q's (Les Berges, Fig. 2a). For a multifractal system, on the other hand, the linear behavior covers a limited range of scales and it changes for different q's (Dusk Red Latosol 1, Fig. 2b) (Voss, 1988).

The heterogeneity of a distribution can also be assessed by the shape of a $f(\alpha)$-spectrum. An homogeneous fractal exhibits a narrow $f(\alpha)$-spectrum (Les Berges, Fig. 3), whereas the opposite is true for an heterogeneous fractal (Dusk Red Latosol 1, Fig. 3). The magnitude of the changes around the maximum values of $f(\alpha(0)) = D_0$ is a measure of the symmetry of a $f(\alpha)$-spectrum. The differences $(D_0 - D_1)$ and $\{f[\alpha(-1)] - D_0\}$ indicate the deviation of the $f(\alpha)$-spectrum from its maximum value ($q = 0$) toward the left side ($q > 0$), and the right side ($q < 0$) of the curve, respectively. The values of the differences $(D_0 - D_1)$, and their corresponding $\{f[\alpha(-1)] - D_0\}$ differences increased with clay

Table 2. Selected parameters from a multifractal analysis of particle-size distributions of the studied soils.

Soils	D_0† ± SSE‡	R^2§	D_1 ± SSE	R^2	α(−1) ± SSE¶	R^2	α(0) ± SSE	R^2
Dusk Red Latosol 1	1.03 ± 0.04	0.988	0.19 ± 0.03	0.968	1.08 ± 0.36	0.997	1.27 ± 0.34	0.987
Dusk Red Latosol 2	1.03 ± 0.05	0.988	0.59 ± 0.04	0.991	1.49 ± 0.36	0.718	1.23 ± 0.05	0.974
Dusk Red Latosol 3	1.02 ± 0.05	0.996	0.48 ± 0.03	0.997	1.16 ± 0.36	0.967	1.27 ± 0.22	0.965
Red Yellow Latosol 1	1.03 ± 0.05	0.988	0.56 ± 0.07	0.983	1.47 ± 0.22	0.933	1.18 ± 0.01	0.999
Red Yellow Latosol 2	1.04 ± 0.05	0.996	0.67 ± 0.02	0.998	1.48 ± 0.14	0.968	1.18 ± 0.06	0.990
Red Yellow Podzolic 1	1.04 ± 0.04	0.990	0.80 ± 0.03	0.991	1.23 ± 0.19	0.928	1.15 ± 0.06	0.989
Red Yellow Podzolic 2	1.03 ± 0.05	0.997	0.91 ± 0.04	0.998	1.15 ± 0.16	0.947	1.10 ± 0.10	0.993
Red Yellow Podzolic 3	1.03 ± 0.04	0.997	0.72 ± 0.04	0.996	1.35 ± 0.11	0.718	1.23 ± 0.03	0.984
Affoltern	1.02 ± 0.04	0.999	1.01 ± 0.01	0.999	1.04 ± 0.07	0.999	1.03 ± 0.05	0.999
Aeugst	1.03 ± 0.04	0.999	0.99 ± 0.01	0.999	1.12 ± 0.06	0.999	1.07 ± 0.10	0.999
Buelach	1.02 ± 0.04	0.999	1.00 ± 0.03	0.999	1.04 ± 0.07	0.999	1.03 ± 0.05	0.999
Les Barges	1.02 ± 0.03	0.999	1.01 ± 0.03	0.999	1.04 ± 0.05	0.999	1.02 ± 0.03	0.999
Mettmenstetten	1.02 ± 0.04	0.999	0.99 ± 0.03	0.999	1.06 ± 0.09	0.999	1.04 ± 0.06	0.999
Murimoos	1.02 ± 0.04	0.999	1.00 ± 0.03	0.999	1.08 ± 0.12	0.999	1.04 ± 0.06	0.999
Obermumpf	1.02 ± 0.05	0.999	0.99 ± 0.02	0.999	1.09 ± 0.15	0.999	1.07 ± 0.11	0.999
Obfelden	1.02 ± 0.05	0.999	0.99 ± 0.05	0.999	1.14 ± 0.20	0.999	1.07 ± 0.10	0.999
Reckenholz	1.02 ± 0.05	0.999	0.99 ± 0.05	0.999	1.15 ± 0.21	0.999	1.07 ± 0.10	0.999
Rheinau	1.02 ± 0.04	0.999	1.01 ± 0.04	0.999	1.05 ± 0.07	0.999	1.03 ± 0.04	0.999
Wetzikon 1	1.00 ± 0.04	0.999	1.00 ± 0.04	0.999	1.07 ± 0.11	0.999	1.04 ± 0.06	0.999
Wetzikon 2	1.02 ± 0.04	0.999	1.00 ± 0.04	0.999	1.08 ± 0.12	0.999	1.04 ± 0.06	0.999
Wuelfingen	1.02 ± 0.05	0.999	0.98 ± 0.05	0.999	1.14 ± 0.20	0.999	1.06 ± 0.09	0.999
Zeiningen	1.02 ± 0.03	0.999	0.99 ± 0.02	0.999	1.14 ± 0.21	0.999	1.07 ± 0.11	0.999
Gladstone	1.02 ± 0.02	0.999	0.98 ± 0.03	0.999	1.01 ± 0.02	0.999	1.03 ± 0.04	0.998
Holmdel	1.02 ± 0.02	0.999	0.98 ± 0.01	0.999	1.13 ± 0.13	0.987	1.05 ± 0.04	0.997
Palouse	1.04 ± 0.05	0.996	0.87 ± 0.02	0.990	1.29 ± 0.53	0.996	1.18 ± 0.36	0.997
Red Bluff	1.02 ± 0.02	0.992	0.68 ± 0.1	0.978	1.06 ± 0.06	0.994	1.09 ± 0.04	0.992
Ryder	1.02 ± 0.02	0.999	0.92 ± 0.03	0.998	1.02 ± 0.06	0.998	1.03 ± 0.04	0.998
Royal	1.04 ± 0.08	0.999	0.77 ± 0.06	0.999	1.13 ± 0.21	0.998	1.09 ± 0.13	0.999
Salkum	1.04 ± 0.04	0.997	1.00 ± 0.02	0.988	1.28 ± 0.31	0.996	1.26 ± 0.30	0.997
Walla Walla	1.06 ± 0.06	0.997	0.97 ± 0.03	0.999	1.61 ± 0.34	0.994	1.24 ± 0.15	0.997

† D_0 is the capacity dimension; D_1 is the entropy dimension.
‡ SSE is defined as the sum of the squared deviations of each observation around the expected value.
¶ α(−1) and α(0) are the Lipschitz-Hölder-exponent for $q = -1$ and $q = 0$, respectively.
§ R^2 is the correlation coefficient.

contents (Fig. 4), indicating that distribution heterogeneity also increases with clay content. The strong asymmetry of the $f(\alpha)$-spectrum of the Dusk Red Latosol 1 (Fig. 3) is the result of the high clay content (81.2%) of this soil concentrated in one measure (0–2.2 μm). On the other hand, the spectrum of Les Barges soil (Fig. 3), with 0.3% clay content, is symmetric as indicated by the similar and small values of the differences $(D_0 - D_1)$ and $\{f[\alpha(-1)] - D_0\}$. Values of $\alpha(-1)$ or $\alpha(0)$ (Table 2) did not show any trend with the content of sand, silt, or clay. The aperture of the $f(\alpha)$-spectrum denoted by the differences $([\alpha(-1) - \alpha(0)]$ and $[\alpha(0) - \alpha(1)]$ was not correlated with any soil separate (data not shown), suggesting that $(D_0 - D_1)$ is the parameter that best represents variations within a PSD.

The relative proportion of sand, silt, and clay affected the scaling properties of $\tau(q)$ vs. q. According to Eq. [7], a linear relationship between $\tau(q)$ and q implies a single fractal system characterized by one scaling exponent (homogeneous fractal). On the other hand, variable slopes in a $\tau(q)$ vs. q relationship are indicative of a multifractal (heterogeneous) system (Machs et al., 1995). A special case of the latter systems is the bifractal distribution, defined by two slopes dominating a $\tau(q)$ vs. q plot (Korvin, 1992). Typically, two nearly linear sections defined trends for $q > 0$ and for $q < 0$ (Fig. 5). Only soils within Group 1, characterized by clay contents <10% and variable sand and silt contents (Fig. 1), exhibited a nearly single linear trend of the $\tau(q)$ vs. q plots (Fig. 5a). The three soils in the Group 2 (<25% silt and variable amounts of sand and clay) exhibited two distinctively different slopes for $q < 0$ and $q > 0$, with very little difference among soils (Fig. 5b). Greater differentiation was obtained among soils in Group 3 (soils with sand content of <20% and variable contents of silt and clay), which had a larger range of variation in clay content than soils in the Group 2 (Fig. 5c). The shape of the $\tau(q)$ vs. q plots suggests that soils in Group 1 are homogeneous fractal, whereas soils in Group 2 and 3 exhibit multifractal behavior. The well-defined slopes in the $\tau(q)$ vs. q plots suggest that two groups of particle sizes are responsible for the scaling properties of PSD, of which the clay-size fraction seems to be dominant.

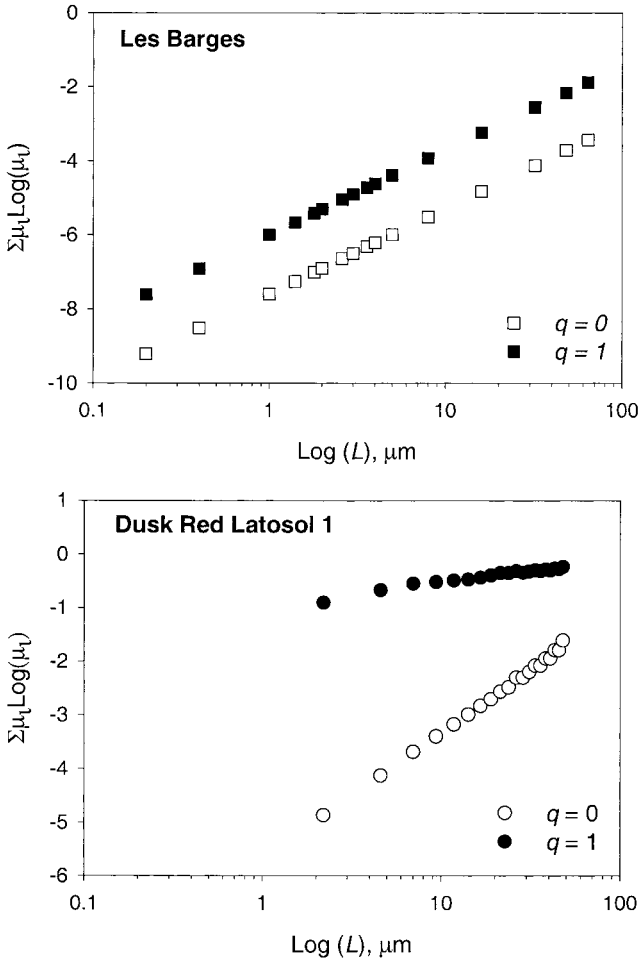

Fig. 2. Plots of $\Sigma_{i=1}^{N(L)} \mu_i(q, L) \log[\mu_i(q, L)]$ vs. log (L) for $q = 0$ and $q = 1$ for the particle-size distributions of (a) the Les Barges, and (b) the Dusk Red Latosol 1 soils. For explanation see text.

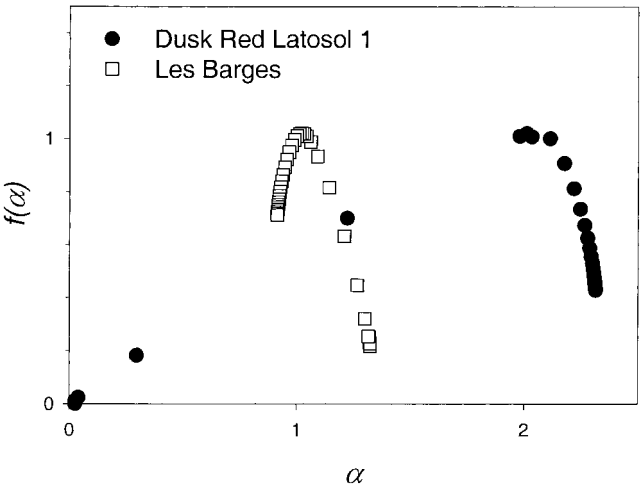

Fig. 3. Example of $f(\alpha)$-spectra for the Les Barges and Dusk Red Latosol 1 soils.

Single and Multifractal Scaling

A single fractal is characterized by the equality of the values of D_0, D_1, and D_2 (see Eq. [9]). Our data show

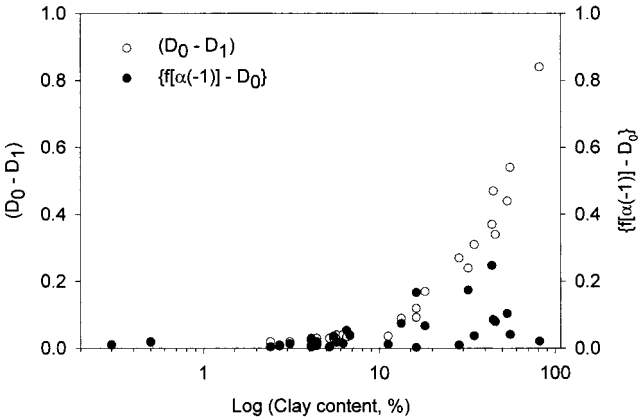

Fig. 4. Plot of differences $(D_0 - D_1)$ and $\{f[\alpha(-1)] - D_0\}$ as a function of clay content.

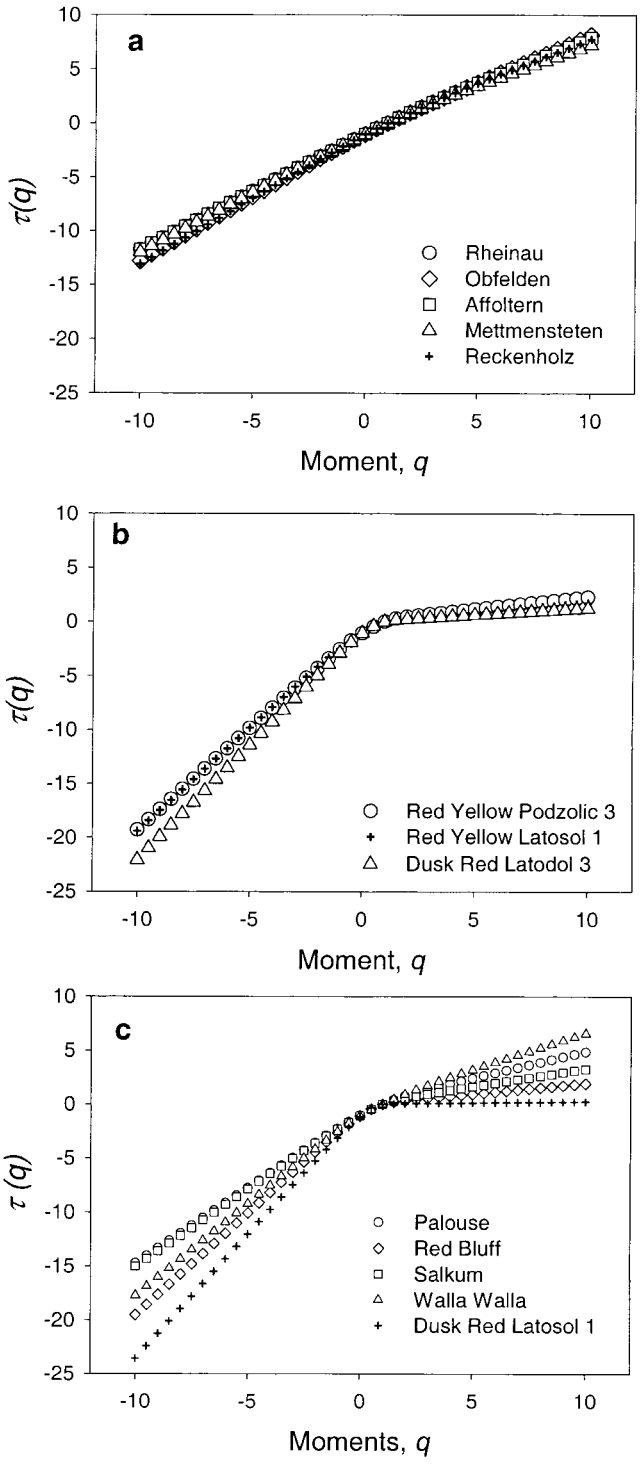

Fig. 5. Plots of $\tau(q)$ vs. q for soil groups shown in Fig. 1, (a) Group 1, (b) Group 2, and (c) Group 3. All soils with clay content <10% exhibited spectra similar to those in Group 1 (data not shown).

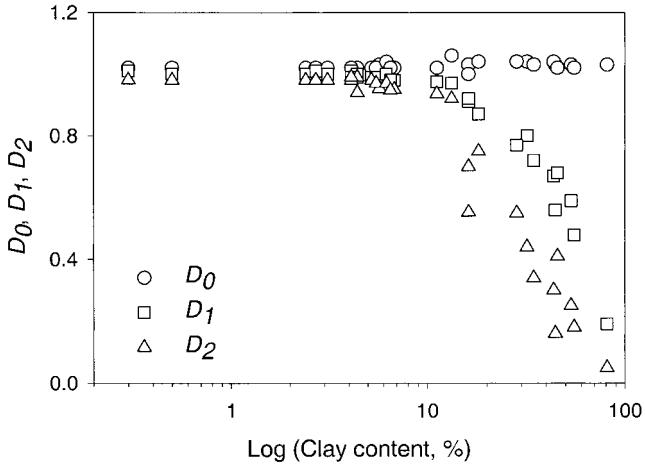

Fig. 6. Plot of the capacity dimension, D_0, the entropy dimension, D_1, and the correlation dimension, D_2, as a function of clay content for all soils.

that this equality occurs for clay contents of <~10% (Fig. 6). For clay increasing beyond 10%, D_0 remains statistically not different from 1.0 ($P < 0.01$), whereas both D_1 and D_2 decrease with increasing clay content. In the region of dissimilar fractal dimensions, the values of D_0, D_1, and D_2 follow the inequality represented in Eq. [9]. A more detailed study is needed to reveal the causes of the scaling properties of soil PSDs, but a hypothesis can be advanced based on changes in entropy in an open system and their effect on a PSD. Soils are open systems tending to steady state conditions characterized by a minimum production of entropy (Addiscott, 1995). Statistically, this means that as the entropy decreases a system becomes more ordered (Smeck et al., 1983). In multifractal systems, the dimension D_1 is directly associated to the entropy of the system (Voss, 1988). Consistent with the interpretation of entropy in an open system, we found that D_1 values decreased as the fraction of clay-sized particles increased above 10% and irregularities concentrate in that size domain (Table 2 and Fig. 6). A predominance of sand is associated with a single fractal dimension representing a random system of greater entropy than one dominated by clay.

Bittelli et al. (1999) and Tyler and Wheatcraft (1992) have reported values of fragmentation fractal dimensions increasing with clay contents, but we believe this to be the first report on the trend of D_0, D_1, and D_2 for soil particle distributions covering a wide range of textural classes.

The results presented in this paper do not invalidate the fractal analyses done in the past, but it suggests that multifractal techniques provide additional information to characterize a distribution. Models based on single fractal are limited to PSDs with clay contents of <10%. Further studies including samples representing all regions of the textural triangle may refine the limits of applicability of single fractal models in soils.

CONCLUSIONS

Multifractal analyses revealed PSDs with single and multifractal scaling. In general, multifractal parameters were related to clay content. A clay content of ~10% separated single from multifractal scaling. A further refinement in such study will be to redefine size boundaries of soil separates (e.g., in the size range between clay and silt) based on their effect on the scaling of a distribution.

The entropy dimension, D_1, is a useful parameter can

be used to distinguish single from multifractal scaling, and the difference ($D_0 - D_1$) constitutes a measure of the degree of heterogeneity of a distribution and may be useful as a predictive parameter.

Models of PSD should recognize differences in scaling properties of particle distributions, and research should be devoted to link these differences with pedogenetic processes to fully interpret the significance and potential of multifractal parameters as a representation of a PSD.

REFERENCES

Addiscott, T.M. 1995. Entropy and sustainability. Eur. J. Soil Sci. 46: 161–168.

Andraud, C., A. Beghdadi, and J. Lafait. 1994. Entropic analysis of random morphologies. Physica A 207:208–212.

Andraud, C., A. Beghdadi, E. Haslund, R. Hilfer, J. Lafait, and B. Virgin. 1997. Local entropy characterization of correlated random microstructures. Physica A 235:307–318.

Appleby, S. 1996. Multifractal characterization of the distribution pattern of the human population. Geographical Analysis 28:147–160.

Beers, Y. 1953. Introduction to the theory of error. Addison-Wesley Publishing Company, Inc., Cambridge, MA

Bittelli, M., G.S. Campbell, and M. Flury. 1999. Characterization of particle-size distribution in soils with a fragmentation model. Soil Sci. Soc. Am. J. 63:782–788.

Buchan, G.D., K.S. Grewal, and A.B. Robson. 1993. Improved models of particle-size distribution: An illustration of model comparison techniques. Soil Sci. Soc. Am. J. 57: 901–908.

Callen, H.B. 1985. Thermodynamics and an introduction to thermostatistics. 2nd ed. John Wiley & Sons, New York, NY.

Cheng, Q., and F.P. Agterberg. 1995. Multifractal modeling and spatial point process. Math. Geol. 27:831–845.

Chhabra, A.B., and R.V. Jensen. 1989. Direct determination of the f(α) singularity spectrum. Phys. Rev. Lett. 62:1327–1330.

Chhabra, A.B., C. Meneveu, R.V. Jensen, and K.R. Sreenivasan. 1989. Direct determination of the f (α) singularity spectrum and its application to fully developed turbulence. Phys. Rev. A 40: 5284–5294.

Evertsz, C.J.G., and B.B. Mandelbrot. 1992. Multifractal measures. p. 921–953. *In* H.-O. Peitgen et al. (ed.) Chaos and fractals. New frontiers of science. Springer-Verlag, New York, NY.

Feder, J. 1988. Fractals. Plenum Press, New York, NY.

Folorunso, O.A., C.E. Puente, D.E. Rolston, and J.E. Pinzon. 1994. Statistical and fractal evaluation of the spatial characteristics of soil surface strength. Soil Sci. Soc. Am. J. 58:284–294.

Gouyet, J.-F. 1996. Physics and fractal structures. Springer-Verlag, New York, NY.

Grassberger, P., and I. Procaccia. 1983. Characterization of strange attractors. Phys. Rev. Lett. 50(5):346–349.

Grout, H., A.M. Tarquis, and M.R. Wiesner. 1998. Multifractal analysis of particle size distributions in soil. Environ. Sci. Technol. 32: 1176–1182.

Halsey, T.C., M.H. Jensen, L.P. Kadanoff, I. Procaccia, and B.I. Shraiman. 1986. Fractal measures and their singularities: The characterization of strange sets. Phys. Rev. A 33:1141–1151.

Hentschel, H.G.E., and I. Procaccia. 1983. The infinite number of generalized dimensions of fractals and strange attractors. Physica D 8:435–444.

Korvin, G. 1992. Fractals models in the earth sciences. Elsevier, Amsterdam, the Netherlands.

Kravchenko, A., C.W. Boast, and D.G. Bullock. 1999. Multifractal analysis of soil spatial variability. Agron. J. 91:1033–1041.

Kropp, J., A. Block, W.V. Bloh, T. Klenke, and H.-J. Schellnhuber. 1994. Characteristic multifractal element distributions in recent bioactive marine sediments. p. 369–421. *In* J.H. Kruhl (ed.) Fractal dynamics systems in geoscience. Springer Verlag, New York, NY.

Liu, H.H., and F.J. Molz. 1997. Multifractal analyses of hydraulic conductivity distributions. Water Resour. Res. 33:2483–2488.

Machs, J., F. Mas, and F. Sagues. 1995. Two representations in multifractal analysis. J. Phys. A: Math. Gen. 28:5607–5622.

Martin, M.A., and F.J. Taguas. 1998. Fractal modelling, characterization and simulation of particle-size distributions in soil. Proc. R. Soc. Lond. Ser. A. 454:1457–1468.

Matsushita, M. 1985. Fractal viewpoint of fracture and accretion. J. Phys. Soc. Japan 54:857–860.

Muller, J., and J.L. McCauley. 1992. Implication of fractal geometry for fluid flow properties of sedimentary rocks. Transp. Porous Media 8:133–147.

Naime, J.M., C.M.P. Vaz, and A. Macedo. 2001. Automated soil particle size analyzer based on gamma-ray attenuation. Comput. Electronics Agric. 31:295–304.

Oliveira, J.C.M., C.M.P. Vaz, K. Reichardt, and D. Swartzendruber. 1997. Improved soil particle-size analysis by gamma-ray attenuation. Soil Sci. Soc. Am. J. 61:23–26.

Shannon, C.E., and W. Weaver. 1949. The mathematical theory of communication. Univ. of Illinois Press, Chicago, IL.

Smeck, N.E., E.C.A. Runge, and E.E. Mackintosh. 1983. Dynamics and genetic modelling of soil systems. p. 51–81. *In* L.P. Wilding et al. (ed.) Pedogenesis and soil taxonomy. I. Concepts and interactions. Elsevier, New York, NY.

Soil Survey Division Staff. 1993. Soil survey manual. USDA Handb. 18. U.S. Gov. Print Office, Washington, DC.

Turcotte, D.L. 1986. Fractals and fragmentation. J. Geophys. Res. 91: 1921–1926.

Tyler, S.W., and S.W. Wheatcraft. 1992. Fractal scaling of soil particle-size distributions: Analysis and limitations. Soil Sci. Soc. Am. J. 56:362–369.

Vaz, C.M.P., J.C.M. Oliveira, K. Reichardt, S. Crestana, P.E. Cruvinel, and O.O.S. Bacchi. 1992. Soil mechanical analysis through gamma ray attenuation. Soil Technol. 5:319–325.

Vicsek, T. 1992. Fractal growth phenomena. 2nd ed. Word Scientific Publishing Co., Singapore.

Voss, R.F. 1988. Fractals in nature: From characterization to simulation. p. 21–69. *In* H.-O. Peitgen and D. Saupe (ed.) The science of fractal images. Springer-Verlag, New York, NY.

Wu, Q., M. Borkovec, and H. Sticher. 1993. On particle-size distribution in soils. Soil Sci. Soc. Am. J. 57:883–890.